



ELSEVIER

Physics of the Earth and Planetary Interiors 103 (1997) 85–100

PHYSICS
OF THE EARTH
AND PLANETARY
INTERIORS

Dynamical effects of a temperature- and pressure-dependent lower-mantle rheology on the interaction of upwellings with the transition zone

Volker Steinbach ^{a,*}, David A. Yuen ^b

^a *Institut für Planetologie, Westf. Wilhelms-Universität, D-48149 Münster, Germany*

^b *Minnesota Supercomputer Institute and Dept. of Geology and Geophysics, University of Minnesota, Minneapolis, MN 55415-1227, USA*

Received 16 September 1996; received in revised form 3 April 1997; accepted 14 April 1997

Abstract

We have examined the consequences of a temperature- and pressure-dependent lower-mantle viscosity on the interaction of upwellings with the two major phase transitions. The viscosity used is only temperature-dependent in the upper-mantle but assumes both temperature- and pressure dependences in the lower-mantle. The activation enthalpy increases with depth dependence scaled after experimental melting curves of lower-mantle components. We have employed a two-dimensional cartesian box with an aspect-ratio of five and a mantle layer thickness of 2900 km, using an extended Boussinesq model with a depth-dependent thermal expansivity. Latent heat release and viscous dissipation have been included in the temperature equation. We have considered models both without and with a viscosity jump (a factor of 8) across the 660 km boundary. The range of averaged Rayleigh numbers (Ra) considered lies between 2×10^6 and 10^7 . A major effect of this temperature- and pressure-dependent rheology is the stabilization of the upwelling plumes and the increase of viscous heating in the bottom portion of these plumes. The impingement of these heated plumes at the endothermic phase boundary causes the development of secondary plumes to rise into the upper-mantle. Shear-heating together with the latent heat release produces large temperature increases in the plumes passing through the transition zone, which may cause melting in the deep upper-mantle. Although the average Rayleigh number in the case of temperature- and pressure-dependent viscosity is around a factor of 5 lower than in a case with purely temperature-dependent viscosity, the resulting flow is only slightly less layered, which is contrary to the earlier finding of Christensen and Yuen (1985). The tendencies for the development of secondary plumes and high temperatures inside the upwellings are enhanced by the viscosity jump at the 660 km boundary. In this situation few nearly steady, vigorous upwellings exist in the lower mantle, while in the upper mantle vigorous time-dependent convection takes place. For an averaged Rayleigh number of 10^7 , the system becomes layered with many thin plumes appearing in the lower mantle. © 1997 Elsevier Science B.V.

Keywords: Lower mantle viscosity; Mantle upwellings; Rayleigh numbers; Upwelling plumes; Temperature and pressure-dependent rheology

* Corresponding author.

1. Introduction

One of the major issues of mantle dynamics, in general, and of possible source regions of mantle plumes in particular is the role played by the transition zone. Plumes must develop from boundary layers, whether from the D' layer or from an internal boundary layer, such as may be formed at the 660 km discontinuity. Studying the nature of the interaction between mantle upwellings and the transition zone is therefore especially relevant. Liu et al. (1991) have pointed out the possibilities for diapirs to be shed from the phase boundary at 660 km depth. Van Keken et al. (1992, 1993) have demonstrated the role played by the changes in the rheological creep law at the 660 km discontinuity on the upwelling flows. Nakakuki et al. (1994) have employed temperature- and pressure-dependent viscosity but within the framework of a Boussinesq model, which does not include the adiabatic and viscous heating terms. Steinbach and Yuen (1994b, 1995) have found strong heating events inside plumes passing through the perovskite to spinel transition by including both viscous and adiabatic heating terms in a temperature-dependent viscous medium. Schubert et al. (1995) have also found intense heating in the plumes due to the coupling between latent-heat release and temperature-dependent viscosity. Recently, Čadež et al. (1995); Schroeder et al. (1995) and Monnereau and Rabinowicz (1996) have demonstrated the importance of depth-dependent viscous stratification on the interaction between major plume upwellings and the mantle phase transitions.

Recent experiments on the melting temperatures of perovskite and other lower-mantle constituents (Zerr and Bohler, 1993, 1994; Shen and Lazor, 1995) have indicated a high melting temperature in the lower mantle. This suggests that a creep law with an activation enthalpy which increases with depth, should be employed for the lower mantle rheology (Van Keken et al., 1994; Van Keken and Yuen, 1995). Previous investigations of this rheology (Van Keken and Yuen, 1995; Van Keken et al., 1995) have only considered Boussinesq models without any phase transitions. In this study, we will extend this type of strongly temperature- and pressure-dependent rheology to study the influences of the two major phase transitions on mantle upwellings. The

dynamical effects of temperature- and pressure dependent rheology are much different from that due to purely temperature-dependent viscosity, especially in the lower mantle. In this vein, we will also investigate the issues concerning the possibility of melting in the transition zone from the thermal-mechanical interaction of the plumes with the phase transition at the 660 km discontinuity, studied earlier with a temperature-dependent viscosity (Steinbach and Yuen, 1994b).

In Section 2, we present the numerical model, the governing equations and the particular lower-mantle viscosity to be used. In the following sections, we report the results for a temperature-dependent viscosity, temperature- and pressure-dependent viscosity and also a model with a viscosity jump at the 660 km discontinuity. We will compare the differences in the dynamics for the various models. We will focus on the thermal fields, as well as the viscous heating and viscosity structures. The paper ends with a discussion of the geophysical implications of this type of lower-mantle viscosity structure on the mantle upwellings across the transition zone (0.5 cm).

2. Model description

The model used here is a two-dimensional cartesian model based on the extended Boussinesq approximation (Christensen and Yuen, 1985). The effects of viscous dissipation and adiabatic heating and cooling are included as well as the release or consumption of latent heat from the phase transitions. The energetics here are different from those employed by Nakakuki et al. (1994); Zhong and Gurnis (1994); King and Ita (1995) and Schubert et al. (1995) in that all of these non-Boussinesq terms in the temperature equation are kept in this formulation. It is important to emphasize here that this approach is self-consistent and emerges from the fully compressible anelastic-liquid approximation (Jarvis and McKenzie, 1980) in the limit $\gamma \rightarrow \infty$, where γ is the thermodynamic Grueneisen parameter. In the compressible formulation, there are two parameters with the dissipation number D present, namely D and D/γ . Physically speaking, in this limit ($D/\gamma \rightarrow 0$) density variations due to compression are neglected,

whereas the thermal effects of compression and expansion are retained. In this extended Boussinesq approach, with only the parameter D present, adiabatic heating and cooling, latent heat release and consumption and viscous heating are balanced. Other approaches, where either adiabatic heating and cooling, latent heat release or viscous dissipation are neglected, are mathematically and physically inconsistent, since all of those quantities scale with the dissipation number D , which governs the scale height of the mantle adiabat. We have compared the results of this approximation with those of an anelastic-liquid model (without phase transitions) in an earlier work (Steinbach et al., 1989) and found very good agreement for dissipation numbers appropriate for the Earth's mantle. Steinbach and Yuen (1995) have also carried out a comparison between this formulation and that in which none of these non-Boussinesq terms are included (e.g., Zhong and Gurnis, 1994). Noticeable differences were found in both the dynamics and the degree of layering.

The derivation of the non-dimensional equations governing convection with phase transitions has been provided in Steinbach and Yuen (1994a). The effects of phase transitions are incorporated by an effective thermal expansivity $\bar{\alpha}$ (Christensen and Yuen, 1985; Steinbach and Yuen, 1994a). It consists of a background portion, which decreases by a factor of seven across the mantle (Chopelas and Boehler, 1992) and an additional 'phase-transition' part, which peaks in the phase-transition regions and is negative for the endothermic spinel \rightarrow perovskite transformation. Clapeyron slopes of 3 and -2.5 MPa/K and relative density changes of 8% and 10% were assumed for the olivine \rightarrow spinel and spinel \rightarrow perovskite transition, respectively.

We have employed the vorticity-stream function approach for a temperature- and pressure-dependent viscous fluid without internal heating due to radioactivity. The main effect of such internal heat sources is an increase in the degree of layering as was pointed out first by Zhao et al. (1992) and later confirmed by Yuen et al. (1994); Solheim and Peltier (1994) and Tackley (1995). The governing equations in the extended Boussinesq framework are:

$$\nabla^2 \psi = \omega \quad (1)$$

$$\nabla^2(\eta\omega) = \bar{\alpha}RaT_x + 2(\eta_{zz}\psi_{xx} - 2\eta_{xz}\psi_{xz} + \eta_{xx}\psi_{zz}) \quad (2)$$

$$\frac{DT}{Dt} - \psi_x \bar{\alpha}D_0(T_0 + T) = \nabla^2 T + \frac{D_0}{Ra} \Phi \quad (3)$$

Here ω , ψ and T denote vorticity, stream function and temperature, respectively, Ra and D_0 the surface Rayleigh and surface dissipation number, T_0 surface temperature and Φ viscous dissipation. The surface dissipation number, D_0 is given by $\alpha_0 gh/C_p$, where α_0 is the surface thermal expansivity, C_p is the heat capacity and g , the gravitational acceleration. As scaling factors for length, time and temperature, we used the depth of the layer, h , thermal diffusion time, h^2/κ_0 (κ_0 being the surface thermal diffusion coefficient) and the temperature drop across the layer, ΔT , respectively. Subscripts x and z indicate partial derivatives, D/Dt total time derivative in the Lagrangian sense. The z -axis points upwards. We used (nondimensional) values of $D_0 = 0.5$ and $T_0 = 0.3$ in all calculations presented in this paper. The dimensionless value of T_0 arises from assuming a dimensional surface temperature of 900 K and a temperature difference across the mantle of 3000 K. The latter value is subject to the largest uncertainty, which may be as big as 800 K. The dimensional temperatures derived in this paper depend both on T_0 and ΔT and thus, have an uncertainty of 200–400 K. We feel, however, that our choice of nondimensional parameters is appropriate to outline the basic physics of the subject of this paper.

We have considered a temperature- and pressure-dependent rheology of the (dimensionless) form

$$\eta = \exp\left(\frac{A}{T_0 + T}\right) \exp\left(-\frac{A_0}{T_0}\right), \quad (4)$$

where

$$A = A_0$$

in the upper mantle and

$$A = A_0 \left(1 + \frac{\Delta\eta(T_0 + T)}{A_0} f(z) + A_1 \frac{z_{670} - z}{z_{670}}\right)$$

in the lower mantle, with

$$f(z) = \frac{1}{2} \left(1 - \tan h\left(\frac{2(z - z_{670})}{d}\right)\right)$$

This form is similar to the rheology employed in Van Keken and Yuen (1995). The second term associated with the definition of A describes a possible jump in viscosity at 660 km depth with a vertical halfwidth of $d = 0.0125$, corresponding to 36 km. In all calculations, $A_0 = 1.27$ was chosen, which means a decrease of viscosity by a factor of 200 due to the temperature difference across the layer alone. In the cases of temperature- and pressure-dependent viscosity, we used $A_1 = 2.5$, which leads to a mean viscosity increase of a factor of 30 to 40 from 660 km depth to the CMB. We note, however, that the increase of viscosity with depth is much larger for cold downwellings than for hot plumes.

The model mantle is 2900 km deep with the endothermic and exothermic phase transitions respectively at 660 km and 400 km depth. A half-width of 36 km has been used in the formulation of the effective thermal expansivity (Steinbach and Yuen, 1994a). All calculations were carried out in a rectangular domain of aspect ratio 5, which is covered by 52 (vertical) by 260 finite elements. Vertical mesh refinement was used to ensure that lower and upper thermal boundary layer and both of the phase transition regions were covered by at least 4 elements or about a $O(10 \text{ km})$ vertical resolution. We have used a constant initial temperature field with error-function profiles in upper and lower thermal boundary and a superimposed perturbation of the form $0.01 \cos(21\pi x) \sin(\pi z)$. Eqs. (1) and (2) were solved with a Galerkin method, while a streamline-upwind Petrov–Galerkin scheme together with a second-order predictor–corrector method was applied to integrate the solution for at least 20,000 time-steps.

As a diagnostic for the degree of layering of the flow, we have used the relative mass flux F (Steinbach and Yuen, 1995) defined here, as the ratio of the root mean square vertical velocity at 670 km depth and the overall root mean square velocity:

$$F = \frac{\left(\frac{1}{l} \int_0^l w^2(x, z_0) dx \right)^{\frac{1}{2}}}{\left(\frac{1}{l} \int_0^l \int_0^1 (u^2 + w^2) dx dz \right)^{\frac{1}{2}}} \quad (5)$$

3. Results

3.1. Purely temperature-dependent viscosity

Steinbach and Yuen (1994b, 1995) and Nakakuki et al. (1994) have employed a temperature-dependent viscosity of the form $\exp(-bT)$ in their studies of convection with phase transitions. The Arrhenius form of the temperature-dependent viscosity $\exp(A/T)$ has been used by Zhong and Gurnis (1994) and Schubert et al. (1995) in their investigation of the influences of the endothermic phase transition in convection. In all of these studies, only the works by Steinbach and Yuen have retained all of the heating terms, such as adiabatic and viscous heating, in the temperature equation.

As a first step, we have turned off A_1 in Eq. (4) to make the viscosity purely temperature-dependent with a viscosity contrast of 200 due to the temperature difference across the layer. Our intention here is to show the difference between purely temperature-dependent viscosity and the temperature- and pressure-dependent lower mantle viscosity to follow. In Fig. 1, we show two snapshots of the temperature field and the associated viscous heating distributions for a surface Rayleigh number of $Ra = 5 \times 10^5$. The Rayleigh number at the bottom is 10^8 and the Rayleigh number based on mean temperature is approximately 10^7 . At the beginning of the integration, convection sets in separately in upper and lower mantle in many small aspect ratio cells. After about 20,000 timesteps, a massive gushing of hot material across the transition zone takes place in the middle of the box. This massive outpour comes from a collective instability from the merging of the small travelling hot plumes at the bottom (first panel of Fig. 1). This super-instability results in fast horizontal hot jets, which then cause flushing events with strong concentration of viscous heating (third panel of Fig. 1) in the descending limb in the upper-mantle. The maximum rate of shear heating is equivalent to about 40 to 50 times the chondritic value. There is also sufficient enough viscous heating in the flushed cold material in the lower mantle to produce halos of hot anomalies next to the descending limbs. After

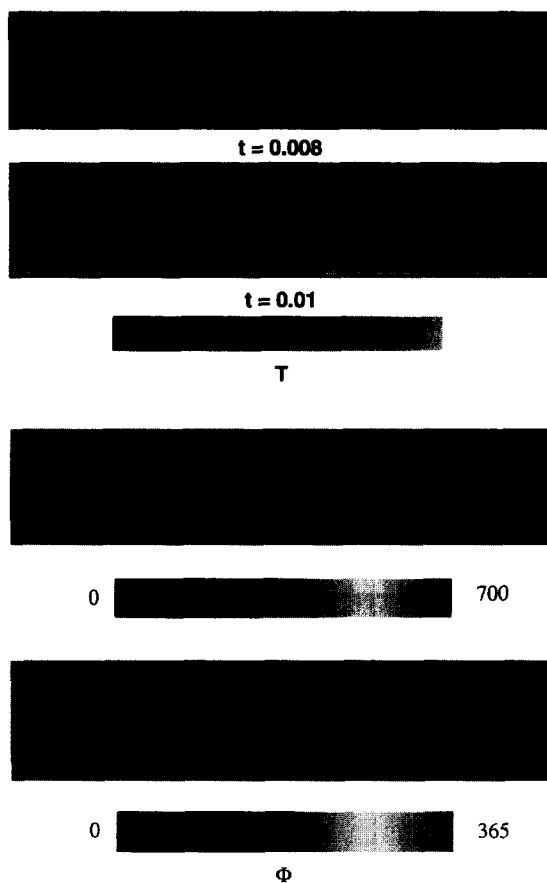


Fig. 1. Convection with purely temperature-dependent viscosity and two phase transitions. The two phase transitions are the olivine to spinel at $z = 0.85$ and the spinel to perovskite at $z = 0.77$. The mantle is 2900 km deep in these models. The viscosity contrast due to temperature across the layer is 200. The surface Rayleigh number is 5×10^5 and 52×260 finite-element grid elements have been used with grid refinement at the two boundary layers and the transition zone with 4 elements in each of the phase transition regions. Each of the phase change has a half-width of 36 km. Top panels show the temperature fields and bottom panels the viscous heating distribution (linear scaling) after around 20,000 and 40,000 timesteps. The maximum rate of 700 for the shear heating corresponds to about 50 times the chondritic heating rate.

40,000 timesteps, the flow exhibits a mixture between layered and non-layered convection (second panel, Fig. 1). Some downwellings from the cold upper boundary layer are blocked by the endothermic phase transition, but there is also a major cold downwelling that penetrates the transition zone down into the lower mantle. The return flow from the lower into the upper mantle (right half of the box) does not come from the CMB, but from rather shallow depths of the lower mantle, as already ob-

served in earlier experiments (Steinbach and Yuen, 1995). The maximum rate of shear heating (bottom panel) has now decreased by a factor of two.

3.2. Temperature and depth-dependent lower mantle viscosity

In this section, we will employ the temperature- and depth-dependent viscosity, given in Eq. (4) in the lower mantle. The viscosity contrast due to temperature is 200 across the mantle and due to depth is

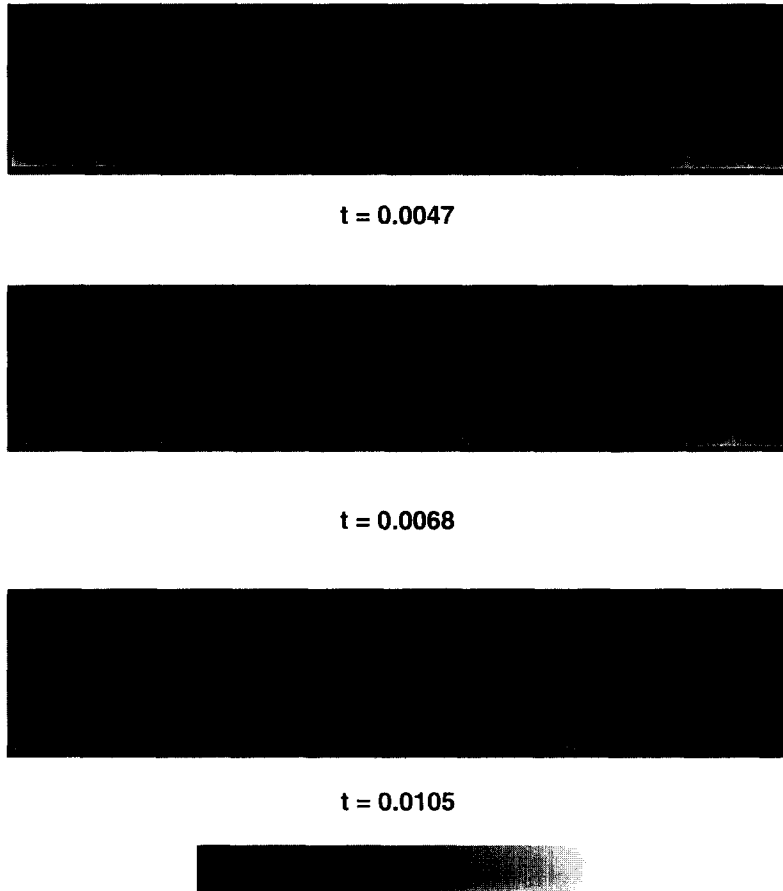


Fig. 2. Temperature fields from convection with a temperature- and depth-dependent lower mantle viscosity and two phase transitions. Otherwise, the same parameters as in Fig. 1. The viscosity contrast due to depth-dependent viscosity across the lower mantle is a factor of around 40. Dimensionless time of 0.001 is equal to 267 Myr.

a factor of 30 to 40 ($A_1 = 2.5$ in Eq. (4)) from the 660 km discontinuity down to the core-mantle boundary (CMB). The surface Rayleigh number is 5×10^5 and the averaged Rayleigh number is around 2×10^6 .

Fig. 2 shows the temperature field for three different time-steps, starting from $t = 0.0047$ or 1.25 Byr to $t = 0.0105$ or 2.8 Byr. From the initial short-wavelength configuration the system undergoes a transition to longer wavelength cells, where only a few plumes are formed at the CMB. These combined dynamical effects arising from the increase of viscosity and the decrease of thermal expansivity with depth have already been reported by Hansen et al. (1993) to occur in a 2-D cartesian model without

phase-transitions. The same phenomenon has been corroborated in 3-D spherical geometries by Zhang and Yuen (1995) and Bunge et al. (1996). It should therefore be interesting to study the consequences of this type of behavior for convection with phase-transitions included.

Due to the increase of viscosity in the lower mantle, the hot plumes emerging from the lower boundary layer become broader and should therefore more easily penetrate the endothermic phase transition region than the rather narrow plumes in the case with purely temperature-dependent viscosity (Tackley, 1995). The initially layered state (top panel) should therefore be much more unstable than in the first case and the transition to a less layered flow

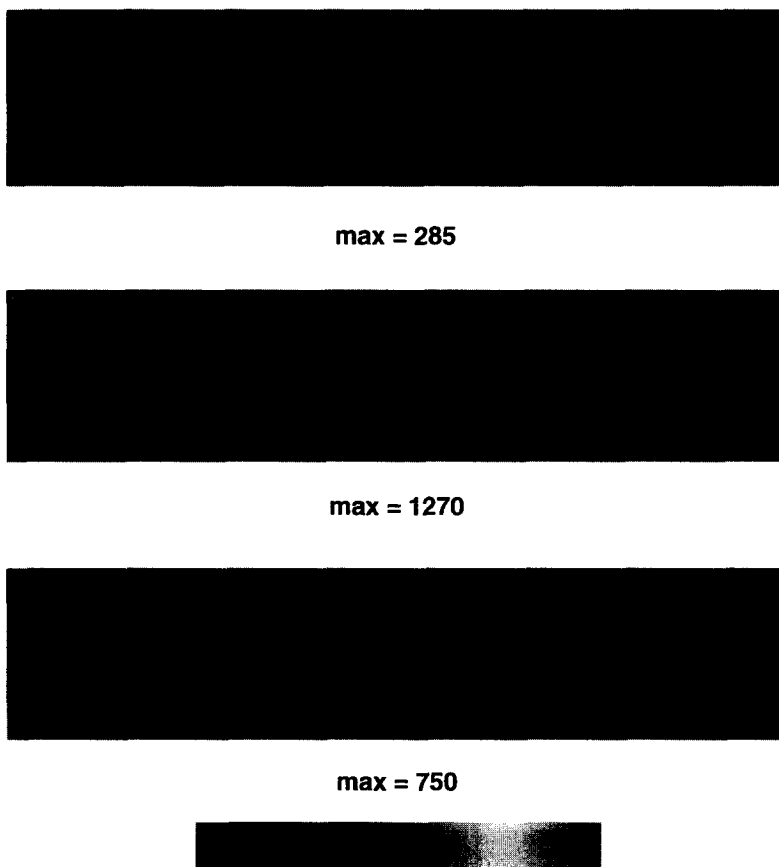


Fig. 3. Viscous heating distribution associated with the temperature fields in Fig. 2. Color bar is scaled linearly.

much more vigorous. But in contrast, this transition takes place more gradually. There is no dramatic global flushing event as shown in Fig. 1. Instead, mass exchange between lower and upper mantle occurs locally (left half side of middle panel) and during several events. This behavior may be explained by the fact that the hot plumes are rather stationary and do not merge into a 'superplume' which may trigger such a big flush event.

The amount of layering of the final states (bottom panel) of the two cases is comparable (see also Fig. 3). The plumes emanating from the CMB have a rather large base, but are thinned out by the focusing effect of the strong gradients of viscosity and thermal expansivity (Van Keken and Yuen, 1995; Hansen et al., 1993) and thus, do not have enough buoyancy to penetrate the transition zone. We should stress here that a simple uniform increase of lower mantle

viscosity will not produce the same focusing effect (Van Keken et al., 1992). Thus, we find here a situation which somehow contradicts the well-known and generally accepted results of Christensen and Yuen (1985): The combined effects of depth-dependent thermal expansivity and temperature- and pressure-dependent viscosity lead to a decrease of the Rayleigh number in the lower mantle by a factor of 5, but the transition from layered to semi-layered flow is less dramatic and the degree of layering of the final flow is similar.

The panels shown in Fig. 2 represent a hybrid form of convection, in which some of the up- and downwellings penetrate the phase transition region and others are blocked at 660 km depth, a scenario similar to that observed by Tackley et al. (1993) in a 3-D spherical model. A new observation is the possible formation of secondary plumes in the transition

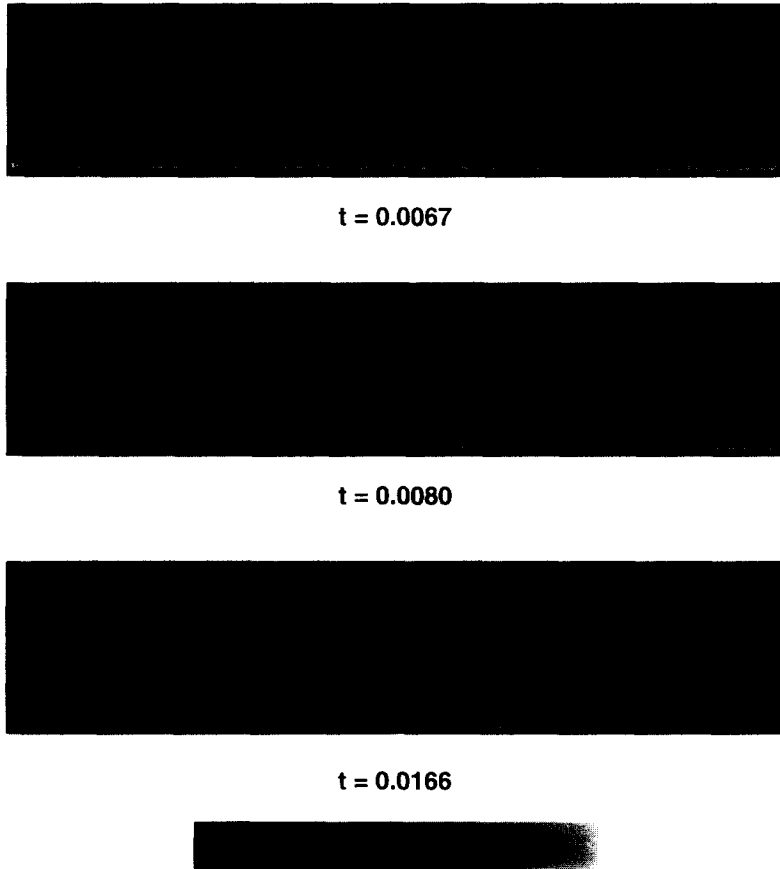


Fig. 4. Temperature fields from convection with a temperature- and depth-dependent lower mantle viscosity, a viscosity jump at 660 km phase boundary and two phase transitions. A viscosity jump by a factor of 8 has been used. Otherwise, the same parameters as in Fig. 1.

zone (middle panel of Fig. 2). Those plumes are much narrower than their 'mother' plumes in the lower mantle and may be shifted horizontally. Since they draw their material from the shallow lower mantle, their appearance makes the transition zone a possible candidate for the source region of ocean island basalts (Allegre and Turcotte, 1985).

A variety of possible behaviour of cold instabilities from the upper mantle is most vividly illustrated in the bottom panel of Fig. 2. Large instabilities are able to penetrate the endothermic phase transition immediately (right hand side), whereas smaller ones are either blocked completely (left hand side) or are deflected horizontally before they sink into the lower mantle (middle).

Upon hitting the phase transition there is a strong interaction between the plume and the phase transi-

tion, as evidenced by the viscous heating produced during the plume impingement on the 660 km boundary (see Fig. 4). The corresponding frames displaying the viscous dissipation distribution are shown in Fig. 4. There is intense viscous heating in both the plumes rising through the upper-mantle (top panel Fig. 4) and sinking currents (middle panel Fig. 4). Viscous heating is largest during a flush event (middle panel Fig. 4), where a maximum heating rate equivalent to around 100 times the chondritic value (Leitch and Yuen, 1989) is associated with the descending flushing current. Obviously, peak dissipation rates are found in the upper thermal boundary layer because of the increase of viscosity leading to large stresses (Zhang and Yuen, 1996; Tackley, 1996). The effects of introducing weak zones here to simulate plate-like behaviour has been discussed by

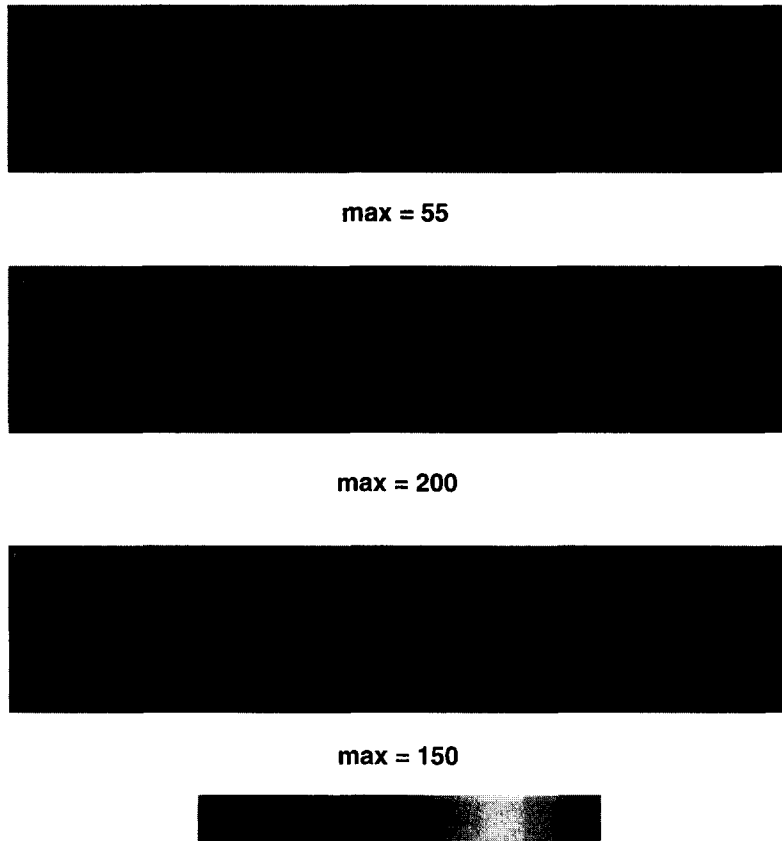


Fig. 5. Viscous heating distribution associated with the temperature fields in Fig. 5.

Zhong and Gurnis (1994) and King and Ita (1995) with Boussinesq models and with non-Newtonian models by Van den Berg et al. (1991). We want to point out here the lower, but still appreciable viscous heating rates in the transition zone, which have been shown to be important in conjecture with latent heat release at 660 km (Steinbach and Yuen, 1994b, 1995).

The effects of a viscosity jump at the 660 km discontinuity are illustrated in Figs. 5 and 6 where a viscosity jump of a factor of 8 has been imposed in Eq. (4). The other parameters, such as the surface Rayleigh number and the two rheological parameters A_0 and A_1 in Eq. (4), remain the same as for the previous case shown in Figs. 2 and 4. With the introduction of $\Delta\eta = 8$, there is a dramatic change in the plume structure and the manner of interaction with the 660 km phase transition. The hot plumes in the lower mantle become much more stationary and

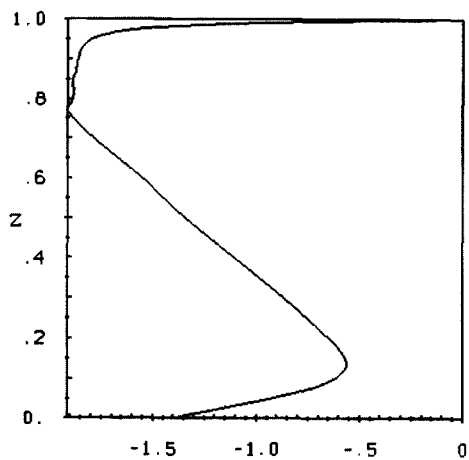
grow wider due to the overall increase in viscosity. The resulting long-wavelength signature of convection in the lower mantle is in agreement with the results of Bunge et al. (1996) and Zhang and Yuen (1996), who used 3-D spherical models with viscosity stratification, but without phase transitions. Secondary hot plumes also form in the transition zone, but they are even narrower than those in Fig. 2 and are shifted farther away from their 'mother' plumes. In contrast to the previous case, no massive downwellings that penetrate into the lower mantle can be observed. A few narrow cold instabilities are deflected at 660 km immediately but then seem to sink further on very slowly. Intense viscous heating is found from the plume impingement and also along the descending limbs (Fig. 6), although the peak rates of viscous dissipation are much lower than in Fig. 4.

In Fig. 7a,b we show the viscosity field and the



log η

$\eta = 100$ $\eta = 0.42$

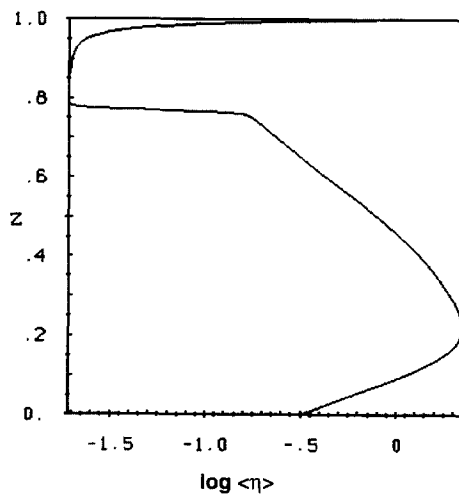


(a)



log η

$\eta = 100$ $\eta = 0.2$



(b)

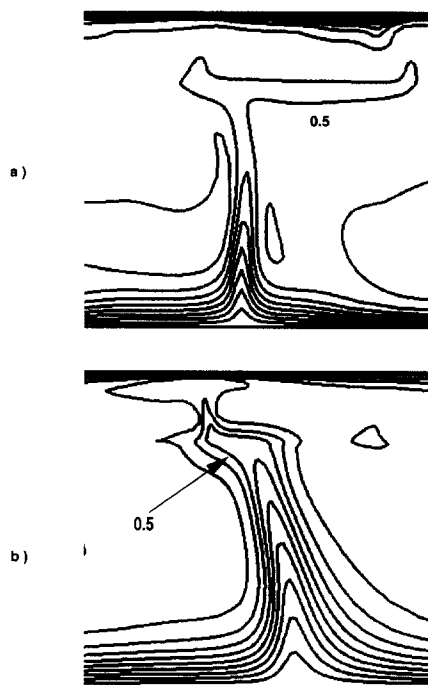


Fig. 7. Close-up shots of individual upwellings in Fig. 2 Fig. 5. (a) Without viscosity jump, (b) with viscosity jump. Spacing between isotherms is equal to 0.07. Total temperature drop ($T = 1$) across the mantle is 3000 K with the surface temperature 900 K.

horizontally averaged profile for the last timesteps shown respectively in Figs. 2 and 5. Characteristic features of both of the viscosity profiles are a low-viscosity upper mantle, a gradual increase of viscosity by two orders of magnitude in the lower mantle and a decrease by a factor of 8 down to the CMB. The viscosity profile shown in Fig. 7b in shape as well as in magnitude resembles those predicted by recent studies in precession constant (Mitrović et al., 1994) and geoid studies (Forte et al., 1995). Introduction of the viscosity jump of course leads to an overall increase of the lower mantle viscosity by a factor of 8, but also increases the thickness of the thermal boundary layer at the CMB, which may be related to the D'' layer, from 400 to 600 km.

Inspection of the viscosity fields shows that there is a low viscosity zone in the phase transition region due to the amount of heat generated by both viscous

heating and latent-heat release from the perovskite to spinel transition. The viscosity here may be by a factor of two lower in the case with the viscosity jump, which may explain the fact that the secondary plumes emerging from this area are much narrower in this case, as can be observed in Fig. 5. There is a dramatic lateral viscosity contrast between the lower mantle plumes and the adjacent lower mantle. Profound differences in the viscosity field are produced by the introduction of the viscosity jump at the 660 km discontinuity. This difference in turn produces an impact on the style of convection in the lower mantle and the dynamics at the transition zone from descending currents and upwelling plumes.

Steinbach and Yuen (1994b) have raised the possibility for local melt generation in the transition zone by the thermal–mechanical interaction between plumes and the 660 km phase transition. There is a growing consensus that komatiites formed in plumes rather than along spreading ridges (Herzberg, 1995) from studies of melting dynamics and phase equilibria of komatiites. Significantly, these experimental results appear to show a secular decrease of the melt segregation depth throughout geological time. In Fig. 8, we zoom into the two plumes shown in Figs. 2 and 5 and examine in closer detail the possibilities for melt to be generated by these large plumes as they pass through the transition zone. Fig. 8a,b shows respectively plumes taken from cases without and with the viscosity jump at the 660 km discontinuity. In both cases very high temperatures are reached by the plume in the transition zone, as shown by the $T = 0.5$ contour, which corresponds to about 2400 K. In the case with viscosity jump (Fig. 8b), the contours associated with $T = 0.36$ (around 2000 K) and $T = 0.43$ (around 2200 K) reach into the upper-mantle and would cause melting. The extra boost in accelerating the plume across the viscosity jump would further facilitate melt generation in the upper mantle. All dimensional temperatures are given here with an uncertainty of 200–400 K, which mainly comes from the uncertainty about the temperature difference across the mantle that may be as big as 800 K.

Fig. 6. Viscosity field and profile for temperature- and depth-dependent viscosity convection with two phase transitions. (a) Without viscosity jump, (b) with viscosity jump. The viscosity fields are taken from the last time-frame shown in Figs. 2 and Fig. 5.

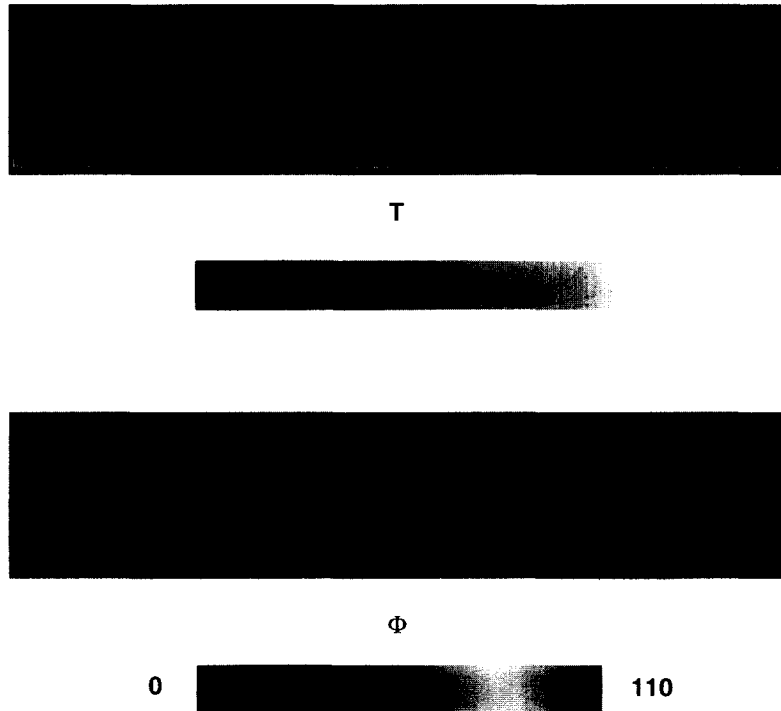


Fig. 8. Temperature and viscous dissipation fields for high Rayleigh number. The surface Rayleigh number is 2×10^6 and the averaged Rayleigh number is close to 10^7 . Over 18,000 timesteps have been integrated for obtaining this frame.

The effects of increasing Ra are shown in Fig. 9, where the surface Rayleigh number has been raised to 2×10^6 and the averaged Rayleigh number is close to 10^7 . We have taken the same viscosity relationship used in Fig. 2, i.e., without any viscosity jump across the 660 km phase boundary. It is well known that convection with an endothermic phase transition has a propensity toward layering with increasing Rayleigh number (e.g., Christensen and Yuen, 1985; Zhao et al., 1992 and Steinbach et al., 1993). Indeed, a strong layering between the upper- and lower-mantle circulations takes place. The number of lower-mantle plumes increases at this higher Ra and they are unable to merge successfully to a larger plume, which may penetrate the 660 km boundary. We see the evidence of small secondary plumes developing off the endothermic phase boundary and generating some viscous heating in the process (bottom panel of Fig. 9). Viscous heating is strongest along the descending flows in the upper mantle, although trails of heating are still discernible along the lower-mantle upwellings.

The mass flux is a quantity, which measures the amount of mass transport across a given depth. We have introduced the relative mass flux $F(z)$ (Steinbach and Yuen, 1992) as the ratio of the root mean square vertical velocity at the depth of the endothermic phase boundary and the global root mean square velocity (see Eq. (5)). Fig. 3 shows the mass flux vs. depth averaged over the last 1000 time-steps of the cases displayed in Figs. 1–3 and 5. The local minimum at $z = 0.77$ is due to the blockage of mass transfer enforced by the endothermic phase transition and can be observed in all four cases. Comparison of the results in terms of degree of layering is difficult: The absolute value of F taken by itself does not serve as a good indicator for layering, since this quantity is scaled by the mean flow velocity. Obviously, the ratio of the maximum and minimum of F is a measure of the deceleration of the vertical flow and hence a better indicator for the degree of layering. Clearly, the high Rayleigh number case (Fig. 3d) exhibits the highest degree of layering, but comparison of the first three cases is still ambiguous: If

we compare the ratio of the maximum of F in the lower mantle and F at $z = 0.77$, i.e., the deceleration of lower mantle flow, the case with purely temperature-dependent viscosity is the most layered one (Fig. 3a), followed by the second (b) and the third case (with viscosity jump, (c)), which shows no layering at all. But in terms of deceleration of upper mantle flow, the last case shows strongest layering, while the first and second are comparable. Nevertheless, we believe that an examination of the temperature fields in Figs. 1, 2 and 5 shows that the first two cases exhibit a similar amount of layering while the flow with a viscosity jump is of more whole-mantle type, since in this case coherent thermal structures aligned vertically are found over the whole mantle.

In Fig. 10, we monitor the corresponding time-histories of the mass flux at the 660 km boundary. Clearly, the high Rayleigh number case (Fig. 10c) after an initial transient remains layered for a long time with small fluctuations. On the other hand, at lower Rayleigh number a significant amount of mass

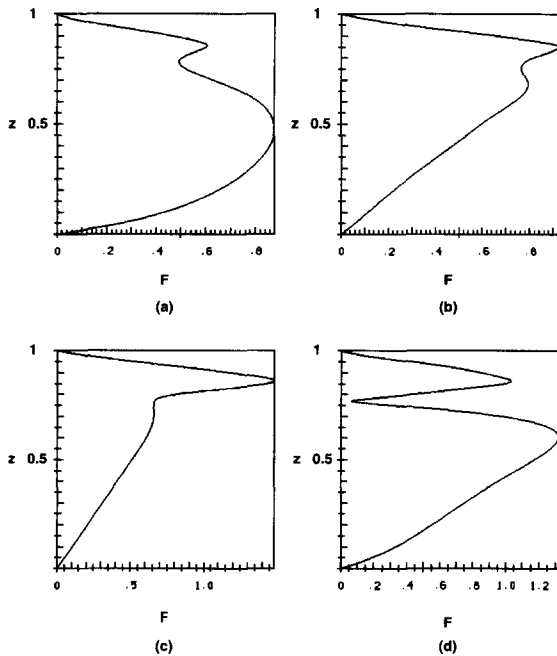


Fig. 9. The vertical mass flux as a function of depth for four cases, averaged over the last 1000 timesteps, (a) urely temperature-dependent viscosity, (b) temperature- and pressure-dependent viscosity, no viscosity jump, (c) with viscosity jump and (d) with high Ra. The definition for the mass flux is given in Eq. (5).

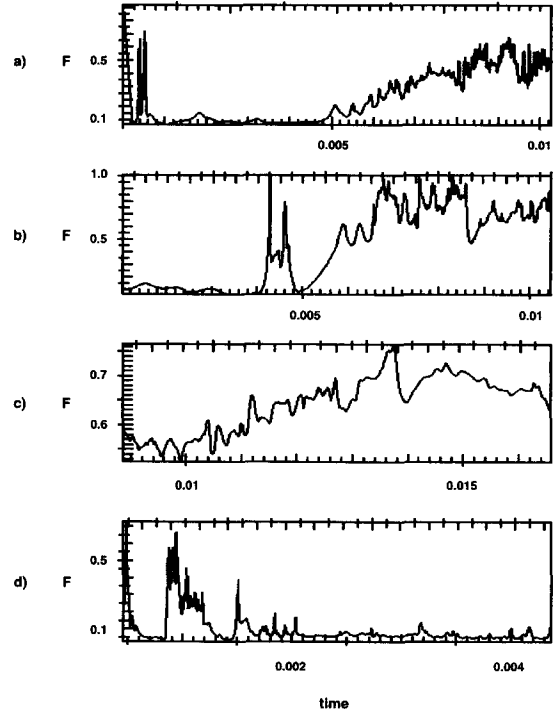


Fig. 10. The time-series of the vertical mass flux at the 660 km boundary for the four cases presented in Fig. 3.

transfer, $F > 0.5$, across the 660 km occurs with irregular fluctuations.

4. Summary and geophysical implications

We have examined the dynamical ramifications on phase transitions due to the temperature- and pressure-dependent rheology implied by the experimentally measured melting curves of lower-mantle constituents (Zerr and Boehler, 1993, 1994). There is a stark contrast in the dynamical behavior between plumes with purely temperature-dependent viscosity (Steinbach and Yuen, 1994b; Schubert et al., 1995) and those with this type of temperature- and pressure-dependent lower-mantle viscosity. In calculations with purely temperature-dependent viscosity, collective instabilities from the CMB tend to form a superplume, which may then penetrate the transition zone and cause a catastrophic flushing event. Although the combined effects of depth-dependent

thermal expansivity and temperature- and pressure-dependent viscosity produce a smaller Rayleigh number in the lower mantle, the transition from layered to semi-layered convection is less dramatic. The degree of layering of the final states is comparable, which is paradoxical according to the conventional idea that a higher Rayleigh number enhances layering (Christensen and Yuen, 1985).

Temperature- and pressure-dependent viscosity leads to a hybrid-type of circulation, where unlayered and layered convection patterns can coexist. In this scenario, there is a tendency for secondary plume instabilities to be developed in the transition zone. These secondary plumes are much narrower than their 'mother' plumes in the lower mantle, especially for models with a slight viscosity contrast across the 660 km boundary. As they draw their material from the top portion of the lower mantle, they may be potential hotspot sources.

Comparison of the mass flux quantity and the plume structures indicates that a viscosity increase across the 660 km boundary actually helps to promote whole mantle-type of circulation. This new result can be interpreted as a threshold type of phenomenon, in which the flow would react to the imposed constraint, that of a viscosity jump, with greater vigor than otherwise. Similar behavior has also been found by Hansen and Yuen (1994) in looking at the effects of decreasing thermal expansivity in promoting breakthrough type of events in thermal-chemical convection. Monnereau and Rabinowicz (1996) and Schroeder et al. (1995) have found a similar type of threshold behavior for phase transitional convection with a depth-dependent viscosity.

There are significant flow differences between the upper and lower mantle, as in the situation without any phase transitions (Van Keken and Yuen, 1995). This difference is enhanced with the viscosity jump across the 660 km discontinuity. The presence of the viscosity jump raises the depth of the local viscosity maximum in the lower mantle and increases the overall lower-mantle viscosity. The lowest viscosity in the system is found right above the 660 km discontinuity. A few large relatively stationary plumes are found in the lower mantle, while the rest of the lower mantle is being driven by the more vigorous upper mantle flow (Van den Berg and

Yuen, 1996). This type of multiple-scale phenomenon is caused by the strong vertical asymmetry induced by the viscosity and thermal expansivity and now further enforced by the endothermic phase transitions. Viscous heating is found to be localized and to assume maximum values along the descending limbs in the upper-mantle. There is some significant viscous heating at the base of the lithosphere and, to a lesser extent, at the 660 km discontinuity from the plume impingement.

The potential presence of the viscosity jump will also help to reinforce our earlier suggestion (Steinbach and Yuen, 1994b) concerning melt-generation in the transition zone by the interaction between the rising plume and the endothermic phase transition. Higher temperatures are brought up in the plumes from this nonlinear threshold-like interaction with the viscosity jump at the 660 km phase transition. This work underscores the importance of considering realistic lower-mantle rheology, which is both temperature- and pressure-dependent, in issues related to plume dynamics in the transition zone. These results show the importance of including such a type of lower-mantle viscosity in thermal history calculations with core-cooling thermal boundary conditions (Steinbach et al., 1993).

The presence of large stationary lower mantle plumes is one of the main features of our simulations, which were conducted under 100% base-heated conditions. In Boussinesq cartesian systems, the presence of internal radiogenic heat sources would greatly reduce the size and significance of those plumes. Recent numerical studies, however, have shown that internal heat sources in compressible systems act in a nonlinear manner to amplify major upwellings (Zhang and Yuen, 1996; Bunge et al., 1996). There is also seismic evidence for the existence of two major lower mantle upwellings, which seem to have been rather stable for the last billion years (Dziewonski, 1996). Our intention here is to monitor under what conditions large stable plumes exist and how they interact with phase transitions. Similar questions are also being raised concerning the large plume under Tharsis region in Mars (Breuer et al., 1996; Harder and Christensen, 1996).

Although results from such simple cartesian two-dimensional models may have limited significance when applied to a three-dimensional spherical man-

tle, we believe that the basic physics are portrayed quite well, as shown by comparison with three-dimensional cartesian (Yuen et al., 1994) and spherical models (Tackley et al., 1994).

Acknowledgements

We acknowledge stimulating discussions with S. Zhang, T. Nakakuki, and B.S. Schroeder. V.S. was a recipient of a Minnesota Supercomputer traveling grant. This research has been supported by the German DFG and the US National Science Foundation (Ocean Sciences Program). Computations have been carried out through the University of Minnesota-IBM Shared Research Project and the Computing Center of Cologne University.

References

- Allegre, C.J., Turcotte, D.L., 1985. Geodynamic mixing in the mesosphere boundary layer and the origin of oceanic islands. *Geophys. Res. Lett.* 12, 207–210.
- Breuer, D., Zhou, H., Yuen, D.A., Spohn, T., 1996. Phase transitions in the Martian mantle: implications for the planet's volcanic history. *J. Geophys. Res.* 101 (E3), 7531–7542.
- Bunge, H.-P., Richards, M.A., Baumgardner, J.R., 1996. Effect of depth-dependent viscosity on the planform of mantle convection. *Nature* 379, 436–438.
- Čadež, O., Kyvalova, H., Yuen, D.A., 1995. Geodynamical implications from the correlation of surface geology and seismic tomographic structure. *Earth Planet. Sci. Lett.* 136, 615–627.
- Chopelas, A., Boehler, R., 1992. Thermal expansivity in the lower mantle. *Geophys. Res. Lett.* 19, 1983–1986.
- Christensen, U.R., Yuen, D.A., 1985. Layered convection induced by phase transitions. *J. Geophys. Res.* 90, 10291–10300.
- Dziewonski, A.M., 1996. Earth's mantle in three dimensions. In: Boschi, E., Ekstroem, G., Morelli, A. (Eds.), *Seismic Modelling of Earth Structure*. Editrice Compositori, Bologna, Italy, pp. 507–572.
- Forte, A.M., Dziewonski, A.M., O'Connell, R.J., 1995. Continent-ocean chemical heterogeneity in the mantle based on seismic tomography. *Science* 268, 386–388.
- Hansen, U., Yuen, D.A., Kroening, S.E., Larsen, T.B., 1993. Dynamical consequences of depth-dependent thermal expansivity and viscosity on mantle circulations and thermal structure. *Phys. Earth Planet. Inter.* 77, 205–233.
- Hansen, U., Yuen, D.A., 1994. Effects of depth-dependent thermal expansivity on the interaction of thermal–chemical plumes with a compositional boundary. *Phys. Earth Planet. Inter.* 86, 205–221.
- Harder, H., Christensen, U.R., 1996. A one-plume model of martian mantle convection. *Nature* 380, 507–509.
- Herzberg, C.T., 1995. Generation of plume magmas through time: an experimental perspective. *Chem. Geol.* 126, 1–16.
- Jarvis, G.T., McKenzie, D.P., 1980. Convection in a compressible fluid with infinite Prandtl number. *J. Fluid Mech.* 96, 515–583.
- King, S.D., Ita, J., 1995. Effects of slab rheology on mass transport across a phase transition boundary. *J. Geophys. Res.* 100, 20211–20222.
- Leitch, A., Yuen, D.A., 1989. Internal heating and thermal constraints on the mantle. *Geophys. Res. Lett.* 16, 1407–1410.
- Liu, M., Yuen, D.A., Zhao, W., Honda, S., 1991. Development of diapiric structures in the upper mantle due to phase transitions. *Science* 252, 1836–1839.
- Mitrovica, J.X., Pan, R., Forte, A.M., 1994. Late Pleistocene and Holocene ice mass fluctuations and the earth's precession constant. *Earth Planet. Sci. Lett.* 128, 489–500.
- Monnereau, M., Rabinowicz, M., 1996. Is the 670 phase transition able to layer the earth's convection in a mantle with depth-dependent viscosity?. *Geophys. Res. Lett.* 23, 1001–1004.
- Nakakuki, T., Sato, H., Fujimoto, H., 1994. Interaction of the upwelling plume with the phase and chemical boundary at the 670 km discontinuity: effects of temperature-dependent viscosity. *Earth Planet. Sci. Lett.* 121, 369–384.
- Schroeder, B., Yuen, D.A., Seno, T., 1995. Influence of viscosity jump on the formation of megaplumes in the lower mantle and fast hot jets in the upper mantle. *EOS, Trans. Am. Geophys. Union* 76 (46), F634.
- Schubert, G., Anderson, C., Goldman, P., 1995. Mantle plume interaction with an endothermic phase change. *J. Geophys. Res.* 100, 8245–8256.
- Shen, G., Lazor, P., 1995. Measurement of melting temperatures of some minerals under lower mantle pressures. *J. Geophys. Res.* 100, 17699–17713.
- Solheim, L.P., Peltier, W.R., 1994. Phase boundary deflections at 660-km depth and episodically layered isochemical convection in the mantle. *J. Geophys. Res.* 99, 15861–15875.
- Steinbach, V., Hansen, U., Ebel, A., 1989. Compressible convection in the earth's mantle: a comparison of different approaches. *Geophys. Res. Lett.* 16, 633–635.
- Steinbach, V., Yuen, D.A., 1992. The effects of multiple phase transitions on Venusian mantle convection. *Geophys. Res. Lett.* 19, 2243–2246.
- Steinbach, V., Yuen, D.A., Zhao, W., 1993. Instabilities from phase transitions and the timescales of mantle evolution. *Geophys. Res. Lett.* 20, 1119–1122.
- Steinbach, V., Yuen, D.A., 1994a. Effects of depth-dependent properties on the thermal anomalies produced in flush instabilities from phase-transitions. *Phys. Earth Planet. Inter.* 86, 165–183.
- Steinbach, V., Yuen, D.A., 1994b. Melting instabilities in the transition zone. *Earth Planet. Sci. Lett.* 127, 67–75.
- Steinbach, V., Yuen, D.A., 1995. The effects of temperature-dependent viscosity on mantle convection with the two major phase transitions. *Phys. Earth Planet. Inter.* 90, 13–36.
- Tackley, P.J., Stevenson, D.J., Glatzmaier, G.A., Schubert, G., 1993. Effects of an endothermic phase transition at 670-km depth on spherical mantle convection. *Nature* 361, 699–704.
- Tackley, P.J., Stevenson, D.J., Glatzmaier, G.A., Schubert, G., 1994. Effects of multiple phase transitions in a three dimen-

- sional spherical model of convection in earth's mantle. *J. Geophys. Res.* 99, 15877–15902.
- Tackley, P.J., 1995. On the penetration of an endothermic phase transition by upwellings and downwellings. *J. Geophys. Res.* 100 (B8), 15477–15488.
- Tackley, P.J., 1996. Effects of strongly variable viscosity on three-dimensional compressible convection in planetary mantles. *J. Geophys. Res.* 101, 3311–3332.
- Van den Berg, A.P., Yuen, D.A., Van Keken, P.E., 1991. Effects of depth-variations in creep laws on the formation of plates in mantle dynamics. *Geophys. Res. Lett.* 18, 2197–2200.
- Van den Berg, A.P., Yuen, D.A., 1996. Is the lower-mantle rheology Newtonian today?. *Geophys. Res. Lett.* 23, 2033–2036.
- Van Keken, P.E., Yuen, D.A., Van den Berg, A.P., 1992. Pulsating diapiric flows: consequences of vertical variations of mantle creep laws. *Earth Planet. Sci. Lett.* 112, 179–194.
- Van Keken, P.E., Yuen, D.A., Van den Berg, A.P., 1993. The effects of shallow rheological boundaries in the upper mantle on inducing shorter timescales of diapiric flows. *Geophys. Res. Lett.* 20, 1927–1930.
- Van Keken, P.E., Yuen, D.A., Van den Berg, A.P., 1994. Implications for mantle dynamics from the high melting temperature of perovskite. *Science* 264, 1437–1439.
- Van Keken, P.E., Yuen, D.A., 1995. Dynamical influences of high viscosity in the lower mantle induced by the steep melting curve of perovskite: effects of curvature and time dependence. *J. Geophys. Res.* 100 (B8), 15233–15248.
- Van Keken, P.E., Yuen, D.A., Petzold, L.R., 1995. DASPK: a new high order and adaptive time-integration technique with applications to mantle convection with strongly temperature- and pressure-dependent rheology. *Geophys. Astrophys. Fluid Dynam.* 80, 57–74.
- Yuen, D.A., Reuteler, D.M., Balachandar, S., Steinbach, V., Malevsky, A.V., Smedsmo, J.J., 1994. Various influences on three-dimensional mantle convection with phase transitions. *Phys. Earth Planet. Inter.* 86, 185–203.
- Zerr, A., Boehler, R., 1993. Melting of (Mg, Fe)SiO₃-perovskite under hydrostatic, inert conditions to 580 kbar: indication of very high melting temperatures in the lower mantle. *Science* 262, 553–555.
- Zerr, A., Boehler, R., 1994. Constraints on the melting temperature of the lower mantle from high pressure experiments on MgO and magnesiowuestite. *Nature* 371, 506–508.
- Zhang, S., Yuen, D.A., 1995. The influences of lower-mantle viscosity stratification on 3-D spherical-shell mantle convection. *Earth Planet. Sci. Lett.* 132, 157–166.
- Zhang, S., Yuen, D.A., 1996. Various influences on plumes and dynamics in time-dependent compressible mantle convection in a 3-D spherical model. *Phys. Earth Planet. Inter.* 94, 241–267.
- Zhao, W., Yuen, D.A., Honda, S., 1992. Multiple phase transitions and the style of mantle convection. *Phys. Earth Planet. Inter.* 72, 185–210.
- Zhong, S., Gurnis, M., 1994. Role of plates and temperature-dependent viscosity in phase change dynamics. *J. Geophys. Res.* 99, 15903–15918.